



## Mesoscopic study of cylindrical phases of poly(styrene)–poly(isoprene) copolymer: Order–order phase transitions by temperature control

María-del-Rosario Rodríguez-Hidalgo<sup>a</sup>, César Soto-Figueroa<sup>a,\*</sup>, José-Manuel Martínez-Magadán<sup>b</sup>,  
Luís-Vicente<sup>c</sup>

<sup>a</sup>Departamento de Ciencias Químicas, Facultad de Estudios Superiores Cuautitlán, Universidad Nacional Autónoma de México, Av. 1° de Mayo s/n, Campo 1. Cuautitlán Izcallí, 54740 Estado de México, Mexico

<sup>b</sup>Programa de Ingeniería Molecular, Instituto Mexicano del Petróleo, Eje Central Lázaro Cárdenas 152, 07730, D.F. México, México

<sup>c</sup>Departamento de Física y Química Teórica, Facultad de Química, Universidad Nacional Autónoma de México, 04510, D.F. México, México

### ARTICLE INFO

#### Article history:

Received 16 April 2009

Received in revised form

9 July 2009

Accepted 15 July 2009

Available online 21 July 2009

#### Keywords:

Order–order phase transitions

Cylindrical structures

Block polymers

### ABSTRACT

Phase transitions of cylindrical structures of poly(styrene)–poly(isoprene) copolymer (PS–PI) toward spherical and gyroid structures were explored using DPD simulations and a coarse-grained model. Cylindrical phases were first obtained within a composition interval (“predominance region”)  $0.2 < f_{PS} < 0.26$  (volume fraction of poly(styrene)). The predominance region of cylindrical structures was then subject to thermal heating cycles. The thermodynamic instabilities of cylindrical microdomains induce anisotropic composition fluctuations and phase transitions. A transition from the cylindrical phase at low composition limit to a spherical arrangement was observed during the thermal heating process. The cylindrical phase at the intermediate and high composition limit within the predominance region exhibits a transition towards a gyroid arrangement. The phase transition control during thermal heating on the cylindrical phases was governed by small variations in composition. The results are consistent with experimental studies.

© 2009 Elsevier Ltd. All rights reserved.

### 1. Introduction

The phase behaviour of block copolymers under a thermal heating process has been extensively studied, both experimentally and theoretically. Thermally induced phase modification in a block copolymer has an enormous potential to modify the physical properties in these materials. Transition from one ordered phase to another via thermal heating is often called an order–order phase transition [1,2]. Leibler [3] was the first in predicting the phase transitions between different kinds of specific structures of a block copolymer in a weak segregation limit (WSL). According to Leibler's mean-field theory, the phase behaviour (separation, segregation and transformation) depends on the enthalpic–entropic interactions between different polymeric fragments, which had been expressed by the reduced parameter  $\chi N$ , where  $\chi$  represents the Flory–Huggins segment–segment interaction parameter and  $N$  refers to the overall degree of polymerization. Fredrickson and Helfand [4] have extended Leibler's theory to include composition fluctuation effects, in this way in the vicinity of weak segregation

limit the thermotropic phase transitions between different kinds of equilibrium phases of block copolymers can be predicted. Block copolymers form a range of defined phases depending on the length of constituent blocks and thermodynamic interaction between them. It is well-known that the poly(styrene)–poly(isoprene) diblock copolymer (PS–PI) can form equilibrium phases such as alternating lamellae (LAM), body-centred-cubic arrangement (BCC or spheres), ordered bicontinuous double diamond (Gyroid), hexagonally perforated layers (HPL) and hexagonally packed cylinders microdomains (HPC or cylinders) [5]. Order–order phase transitions of PS–PI block copolymer phases have been reported in the past years, specifically the order–order phase transition from cylinders-to-spheres [6–10]. Sakurai et al. [11] have experimentally confirmed the existence of a phase transition between hexagonally packed cylinders (HPC) and body-centred-cubic arrangement of PS–PI system; however, some experimental results on the phase transition from HPC-to-Gyroid in the same system have been reported [12,13] lately. Khandpur et al. [14] have reported the “predominance composition” regions of cylindrical phases of block copolymer PS–PI in their phase diagram. The order–order transitions from cylindrical phases to nearby structures have not been explored in detail in the predominance composition region. Experimental evidences suggest that small variations of compositions of cylindrical microdomains

\* Corresponding author. Tel.: +52 55 91758426; fax: +52 55 91756439.  
E-mail address: [csotof15@yahoo.com.mx](mailto:csotof15@yahoo.com.mx) (C. Soto-Figueroa).

can generate, via a thermal heating process, the order–order transitions from cylinders-to-spheres and cylinders-to-gyroid too. In this work, we explored the phase evolution processes of cylindrical structures of the PS–PI system into the predominance composition region from a mesoscopic point of view using dissipative particle dynamics simulation where the phase evolution stages and the transient ordered states are analysed for each time step.

## 2. Simulation method and coarse-grained model

### 2.1. The DPD method

Equilibrium phase evolution of the cylindrical structures can be analysed by means of Dissipative Particle Dynamics simulations. DPD was first introduced by Hoogerbrugge and Koelman [15,16] and recently improved by Groot et al. [17]. For a thorough account of the DPD method, see Refs [18,19]. In DPD, a particle or bead represents a small segment of a copolymer chain. The basic DPD algorithm is similar to those used in molecular dynamics: the difference is that in addition to the conservative force acting between particles, the total force on a particle  $i$  now also contains a dissipative force and a random force:

$$\mathbf{F}_i = \sum_{j \neq i} (\mathbf{F}_{ij}^C + \mathbf{F}_{ij}^D + \mathbf{F}_{ij}^R) \quad (\text{i})$$

The conservative force  $\mathbf{F}_{ij}^C$  is a soft repulsive force that acts between particles  $i$  and  $j$ . The dissipative force  $\mathbf{F}_{ij}^D$  corresponds to a frictional force that depends both on the position and relative velocities of the particles. The random force  $\mathbf{F}_{ij}^R$  is a random interaction between a bead  $i$  and its neighbour bead  $j$ . All forces vanish beyond a cut-off radius  $r_c$ , which is usually chosen as the reduced unit of length,  $r_c \equiv 1$ .

The  $\mathbf{F}_{ij}^D$  and  $\mathbf{F}_{ij}^R$  forces act as a thermostat which conserves momentum and gives the correct hydrodynamics at sufficiently large time and length scales. They are given by:

$$\mathbf{F}_{ij}^C = \left[ \frac{a_{ij}(1 - r_{ij})\hat{r}_{ij}}{o} \quad \left( \frac{r_{ij} \leq 1}{r_{ij} > 1} \right) \right] \quad (\text{ii})$$

$$\mathbf{F}_{ij}^D = \left[ -\gamma\omega^D(r_{ij})(v_{ij} \cdot \hat{r}_{ij})\hat{r}_{ij} \right] \quad (\text{iii})$$

$$\mathbf{F}_{ij}^R = \left( \sigma\omega^R(r_{ij})\xi_{ij}\hat{r}_{ij} \right) \quad (\text{iv})$$

where  $r_{ij} = |\vec{r}_i - \vec{r}_j|$ ,  $\hat{r} = \vec{r}_{ij}/r_{ij}$ ,  $\gamma$  is the dissipation strength,  $\sigma$  is the noise strength,  $\omega^D(r_{ij})$  and  $\omega^R(r_{ij})$  are weight functions of  $\mathbf{F}_{ij}^D$  and  $\mathbf{F}_{ij}^R$  forces respectively,  $a_{ij}$  is the maximum repulsive force between particle  $i$  and  $j$ . In order for the DPD system to have a well-defined equilibrium state obeying Boltzmann statistics, the equilibrium temperature is defined as  $k_B T = \sigma^2/(2\gamma)$ . This condition fixes the temperature of the system and relates it to the two DPD parameters  $\gamma$  and  $\sigma$  ( $k_B T$  is usually chosen as the reduced unity of energy). The parameter  $a_{ij}$  (henceforth referred to as the bead–bead repulsion parameter or simply as the DPD interaction parameter) depends on the underlying atomistic interactions and is related to the parameter  $\chi$  through [17]:

$$a_{ij} = a_{ii} + \frac{k_B T \chi_{ij}(T)}{0.306} \quad (\text{v})$$

In this expression  $a_{ij}$  is in units of  $k_B T$ . In this way, there is a connection between the molecular character of the PS–PI coarse-grained model and the DPD parameter. In the DPD simulation, the dynamic behaviour of the polymeric system is followed by integration

of the equations of motion using a modified version [18] of the Verlet algorithm [20]. Integration of the motion equations for the PS–PI copolymer generates a trajectory through the system phase from which thermodynamic observables may be constructed from a suitable average. From this information, the phase segregation process, equilibrium phases generation, and order–disorder and order–order phase transitions can be observed.

### 2.2. PS–PI copolymer model

The molecular structure of PS–PI copolymer was built by means of the polymer builder module of Accelrys [21]. The copolymeric molecule contains 300 repetitive units in the main chain and its linear architecture is characteristic for this system. The system molecular weight presents an interval of 20,798–25,842. In our simulation a coarse-grained model constituted by 30 particles connected through harmonic springs replaces the PS–PI copolymer real chain, see Fig. 1. In this work, the quantitative estimate of the bead–bead interaction for coarse-grained model is described by means of the interaction parameter  $\chi$  (calculated using the Flory–Huggins thermodynamic model modified by Fan et al. [22]), Graphic 1 exhibits the interaction parameter  $\chi(T)$  as function of temperature. We must comment that established procedures for mapping between DPD and physical scales and for choosing system temperature are not yet available and so we use Flory–Huggins theory (through the  $\chi(T)$  dependence) to introduce the temperature into the DPD simulations.

All DPD simulations were made with Accelrys DPD package with a reduced parameter  $k_B T = 1$ . According to Ref. [17] for  $\rho = 3$ , an interaction parameter  $a_{ij} = 25 k_B T$  reproduces the compressibility of water. The interaction parameters between species were then chosen as:  $a_{ST-ST} = a_{I-1} = 25$ . When  $\chi(T) > 0$ , (incompatibility between species) we take the temperature dependence  $\chi_{ij}(T) = \chi(T)$ , scaled by the statistical segment  $C_n$ , where  $C_n$  is the characteristic ratio (polymeric segment) [23]. In this way, the equilibrium phase behaviour, structure vs temperature variation has been explored. Equation (v) was obtained by Groot and Warren [17] for moderately long chains,  $N = 1-10$  and at fixed reduced density 3. We have used that relation for chain polymers  $N = 10$  [24],  $N = 20$  [10] and in all cases the composition intervals for HPC and BCC phase are approximately the same. So happens in our present case with  $N = 30$ . Therefore, one important assumption in the next calculations is that equation (v) is valid for  $N = 30$  too.

All DPD simulations were carried out in a cubic box ( $20r_c$ ,  $20r_c$ ,  $20r_c$ ) size, containing a total of 8000 representatives chains, spring constant  $C = 4$ , and density  $\rho = 3$ . The coarse-grained number was maintained constant during the DPD simulations. A total of  $5 \times 10^5$

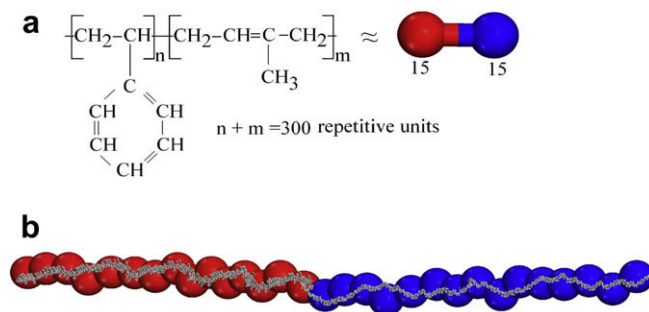


**Fig. 1.** Schematic representation of block copolymer PS–PI: (a) chemical structure of a PS–PI chain,  $n$  and  $m$  represent the polymeric unit number of each block, (b) coarse-grained model of PS–PI system with linear topology. The number of particles of coarse-grained model was determined using the molar mass of block copolymer, molar mass of a repeat unit, degree of polymerization and the characteristic ratio ( $C_n$ ).

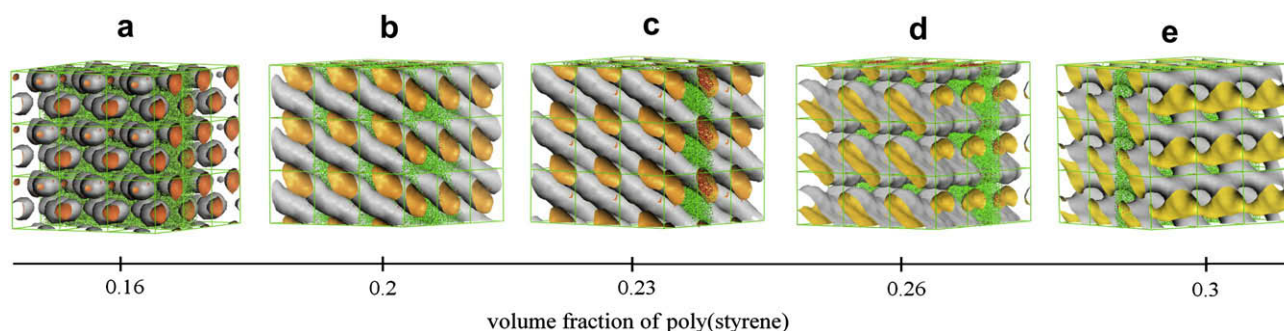


**Fig. 2.** Composition region of equilibrium cylindrical phases of PS-PI copolymer obtained for a  $\chi$  at  $T = 300$  K from Graphic 1 as the block composition (PS/PI) is modified: (a) correspond to spherical structure, (b, c, d) predominance interval of cylindrical phases, and (e) HPL phase.

time steps with step size of  $\Delta = 0.03$  were employed to obtain a reasonable and efficient relaxation for the PS-PI system.

### 3. Results and discussion

All simulations start from a random disordered state, where the copolymer chains PS-PI are in a homogeneous melted phase. The block copolymer can take up an enormous number of configurations by the rotation of chemical bonds into the melt phase and during the thermal relaxation process. To identify the composition specific region where the cylindrical phases are formed, we first scanned the composition interval from 0.1 to 0.5 (volume fraction of poly(styrene) with increments of 0.01). Fig. 2a-e shows the

equilibrium specific ordered structures BCC, HPC and hexagonally perforated layers (HPL) obtained at room temperature (298 K) using the corresponding  $\chi(T)$  from Graphics 1.

The composition region of equilibrium cylindrical phases was so identified to be in the interval  $0.2 < f_{PS} < 0.26$  volume fraction of poly(styrene), Fig. 2b-d. The cylindrical phase behaviour depends on the copolymer molecular weight, styrene-isoprene interaction parameter and their composition. When volume fractions of both block chains are not equivalent, the PS/PI interphase tends to become curve; consequently, the PS/PI interphase becomes more convex toward the minority component as the composition between the poly(styrene) and poly(isoprene) microdomains is more asymmetric [25,26].

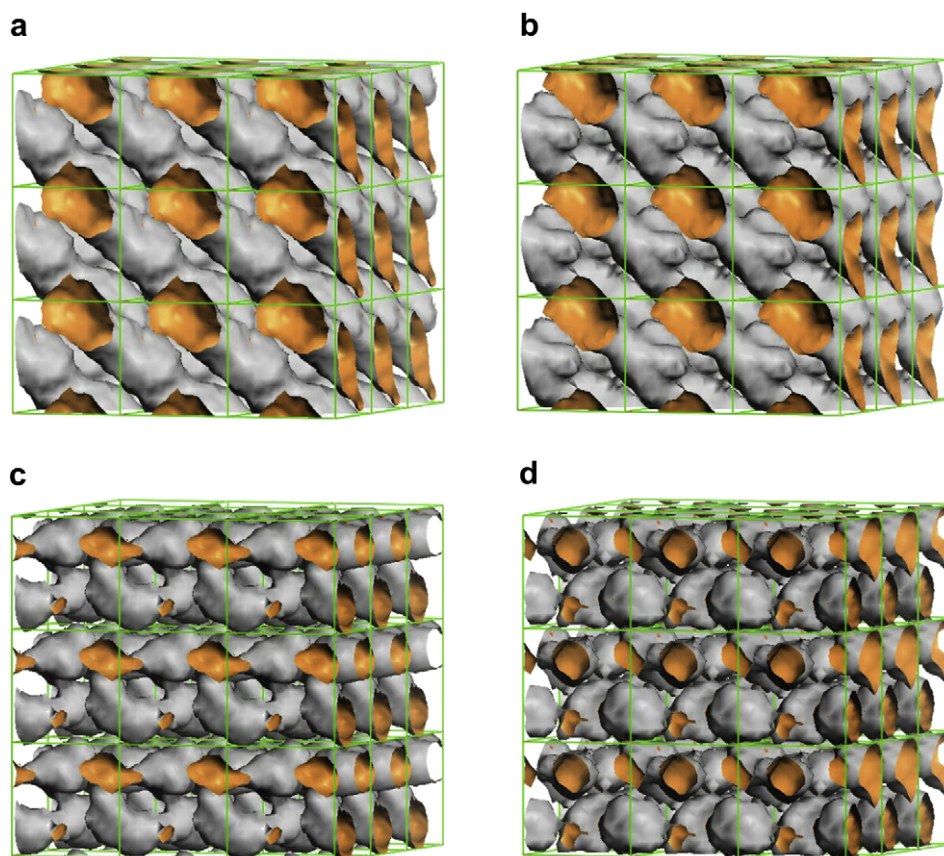


**Fig. 3.** Snapshots of simulations showing the transition process from HPC to spherical arrangement (at the low composition region): (a) undulation process of poly(styrene) microdomains ( $T = 5.3 \times 10^5$ ), (b) breakup of cylindrical phase ( $T = 5.9 \times 10^5$ ), (c) formation of spherical arrangement ( $T = 6.0 \times 10^5$ ) and (d) stabilization of spherical phase ( $T = 1.0 \times 10^6$ ).



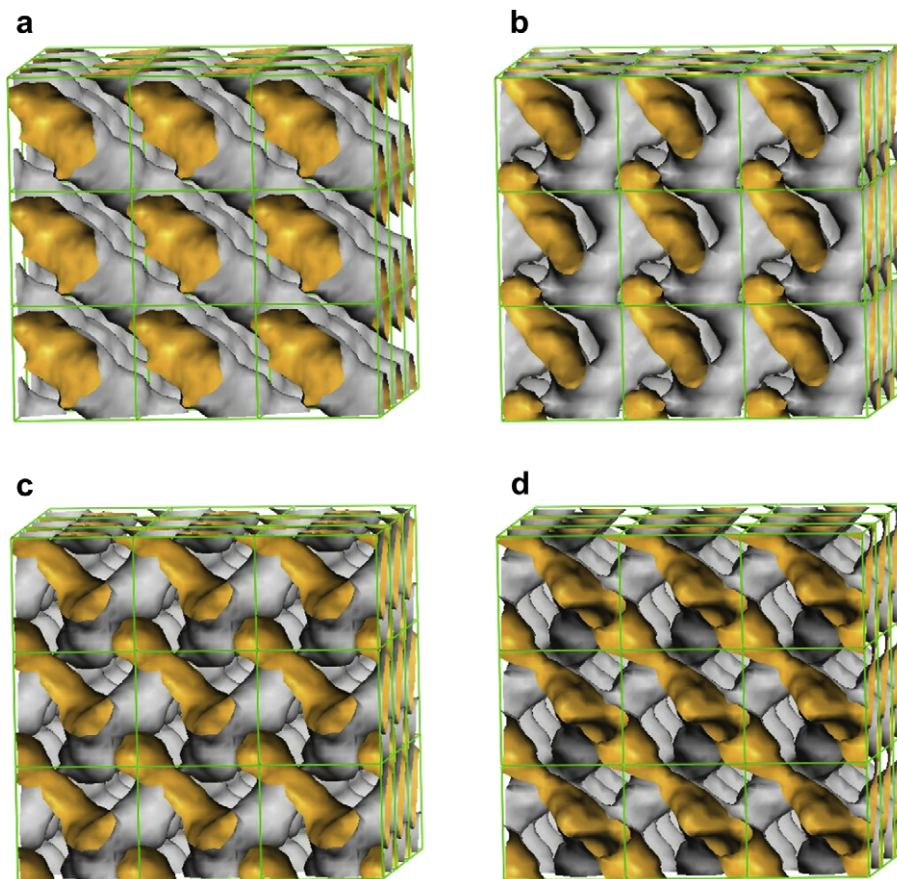


**Fig. 4.** Snapshot of the evolution process during the transition from-HPC-to-Gyroid phase (at an intermediate composition region): (a) undulation process of PS microdomains in the PI matrix by anisotropic composition fluctuations due to heating ( $T = 5.5 \times 10^5$ ), (b) formation of long-lived transient phase of HPL arrangement ( $T = 6.2 \times 10^5$ ), (c) interconnection of HPL phases ( $T = 7.9 \times 10^5$ ) and (d) formation and stabilization of Gyroid arrangement ( $T = 1.0 \times 10^6$ ).

The composition region of the cylindrical phase has two composition limits (low and high composition limit) that are contiguous with other stable phases. In the low composition limit,  $f_{PS} < 0.2$ , the cylindrical phase has as neighbour the BCC arrangement, Fig. 2a–b, whereas in the high composition limit,  $f_{PS} > 0.26$ , the cylindrical structure has as neighbour the HPL phase, Fig. 2d–e. The location of these phases is in accordance with the experimentally determined phase diagram for PS–PI copolymer reported by Khandpur et al. [14].

The possibility of order–order phase transitions of all cylindrical structures of block copolymer PS–PI inside the predominance composition region was explored into the temperature interval from 300 to 600 K. The cylindrical phase can undergo a type of phase modification to produce coexisting intermediate phases that are spatially periodic. It is a well-known fact that the cylindrical phase of PS–PI copolymer can develop long-lived transient or metastable phases during a transition due to energetic barriers and sluggish molecular motion. The intermediate states during the transitions were visualized from a mesoscopic point of view in the DPD simulation.

### 3.1. Order–order phase transition: low composition region

Starting from the equilibrium phase of HPC arrangement with a specific composition of 0.20 (volume fraction of poly(styrene)), the system was annealed at different temperatures and it was verified that they keep the HPC structure and up to a temperature of 452 K the transition from HPC-to-BCC phase was observed. This temperature

marks the transition temperature between phases.  $5.0 \times 10^5$  additional time steps with step size of  $\Delta t = 0.05$  are allowed during the thermal stage to reach the thermodynamic balance of the new arrangement. For our simulation times ( $10^5$  steps) we verified that the system is stable (the fluctuations in reduced temperature are  $0.98 < T < 1.03$ ).

The results show that the transformation from the HPC phase to spherical arrangement by temperature effect proceeds in several stages: (i) undulation of poly(styrene) cylindrical microdomains, (ii) breakup of poly(styrene) cylinders (iii) formation of spherical microdomains and (iv) stabilization of BCC phase, see Fig. 3a–d. This process is induced by the thermodynamic instability of the cylindrical phase, i.e., at the transition point a thermodynamic instability of cylindrical microdomains into poly(isoprene) matrix due to enthalpic and entropic interactions by temperature effects induces anisotropic composition fluctuations [5] and breakup of cylindrical phase in the HPC arrangement and a phase conversion from HPC-to-BCC. The simulation results are in accordance with the experimental outcome reported by Kimishima et al. [8].

### 3.2. Order–order phase transition: intermediate composition region

The HPC phase with a composition of  $f_{PS} = 0.23$  was examined into the temperature interval from 300 to 600 K. The transition from HPC-to-Gyroid arrangement was detected at a temperature of 500 K.

During the annealed process, we observed the long-lived transient phase of HPL arrangement. Four stages were observed during

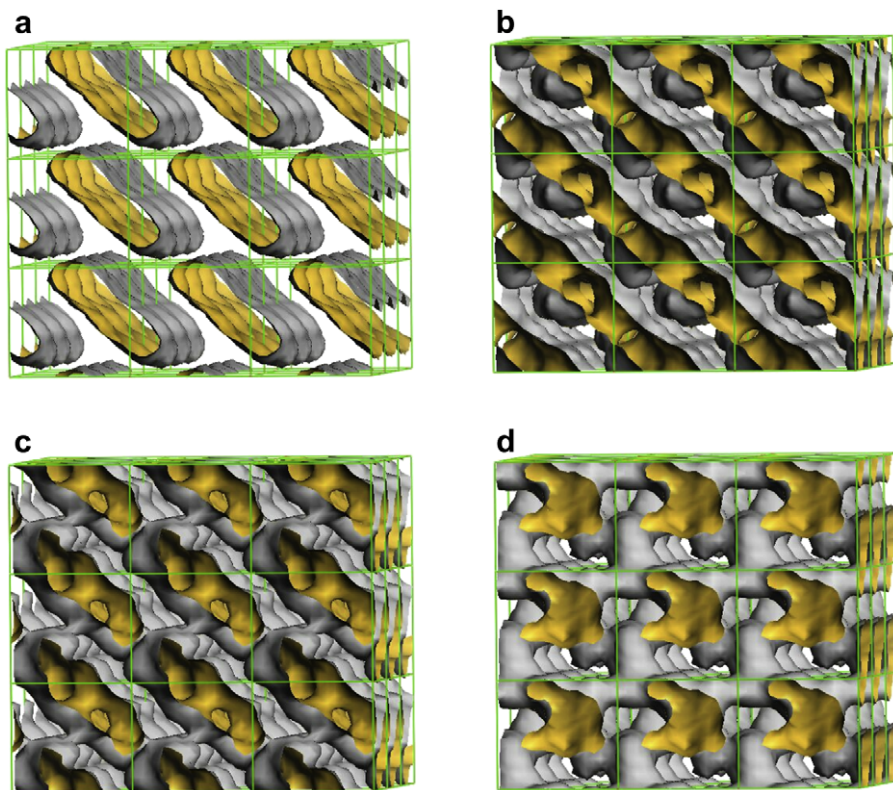


**Fig. 5.** Snapshot of the transition process of cylindrical arrangement (at the high composition region): (a) undulation process of poly(styrene) microdomains ( $T = 5.5 \times 10^5$ ), (b) formation HPL arrangement ( $T = 5.8 \times 10^5$ ), (c) interconnection of HPL phases ( $T = 7.0 \times 10^5$ ) and (d) formation and stabilization of Gyroid phase ( $T = 1.0 \times 10^6$ ).

the transition process: (i) undulation of poly(styrene) cylindrical microdomains, (ii) formation of HPL phase (iii) interconnection of HPL phase (iv) formation and stabilization of gyroid arrangement, see Fig. 4a–d.

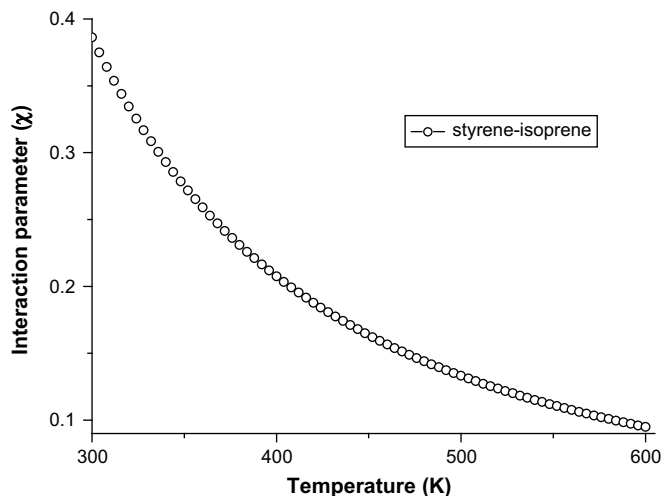
The HPC phase of the composition region of 0.23 (volume fraction of poly(styrene)) showed cylindrical microdomains more dense than the HPC phase of low composition region. The composition increase in the poly(styrene) cylindrical microdomains controls the transition process. Variations of small composition into weak segregation limit (WSL) according to Leibler's mean-field theory greatly modify the phase thermodynamic behaviour (separation, segregation and transformation) [3]. In this way, the enthalpic-entropic interactions between different polymeric microdomains play a main role in the transition process.

When the HPC phase was annealed up to the transition temperature, the thermodynamic instability of cylindrical microdomains by temperature effect undergoes a continuous undulation process. The poly(styrene) cylindrical microdomains avoid their breakup due to their composition (more dense), however, the cylindrical phase gains conformational entropy and tends to expand along the direction parallel to the PS/PI interphase with their neighbours, generating interconnections among them. In this stage, the long-lived transient phases of HPL arrangement are generated. The HPL phases are unstable to an temperature raise, and the anisotropic composition fluctuations between poly(styrene) microdomains promote the formation of interconnections among them; ordered bicontinuous double diamond phases or gyroid evolve then.

### 3.3. Order–order phase transition: high composition region

The cylindrical phase at the high composition limit (composition around 0.26) of the predominance interval lost their HPC

characteristic arrangement (hexagonal packed) due to an increase of the poly(styrene) chains into the cylindrical microdomains. The cylindrical phase changes its orientation with respect to compositions  $f = 0.2, 0.23$ , and the cylinders volume increase, see Fig. 2d. This arrangement was annealed up to a temperature of 540 K; we observed now the transition of cylindrical arrangement to a gyroid phase. The results show that the transformation from the cylinder arrangement to the gyroid phase by temperature proceeds in several stages similar to the observed in the HPC arrangement of intermediate composition region, see Fig. 5a–d. The Fig. 5a shows the initial cylindrical configuration, Fig. 5b and c



**Graphic 1.** Interaction parameters ( $\chi$ ) vs temperature.

shows the connection between the cylinders. Finally, Fig. 5d, shows the final gyroid phase obtained at the end of the simulation.

#### 4. Conclusions

Phase transitions from the cylindrical structure shown by the diblock copolymer PS-PI inside the composition region,  $0.2 < f_{SI} < 0.26$ , were explored through DPD simulations. Thermally induced phase modification on the cylindrical arrangements shows order–order phase transitions from HPC-to-BCC in the low limit and from HPC-to-Gyroid arrangement at intermediate and high composition limits. The control of phase transition during thermal heating was governed by composition small variations in the poly(styrene) cylindrical microdomains. Thermodynamic interactions and the composition fluctuations between the PS and PI pure microdomains are affected by poly(styrene) phase density increase and therefore the directionality of the transition is modified too. The results are consistent with experimental studies and provide a test to predict and control transitions of more complex phases. A final remark concerning the connection between temperature and dissipation in DPD: the increase of the temperature leads not only to better mixing of PS and PI units, which is reflected in reduction of the parameter  $\chi$  (Graphic 1), also to faster dynamics, via the random force coefficient  $\sigma$  in equation (iv). Because the equilibrium temperature is defined as  $k_B T = \sigma^2 / 2\gamma$ , changing  $k_B T$  implies changing the relationship between  $\sigma$  and  $\gamma$ . We have verified that by changing  $0 < k_B T < 2$  (reduced units), which changes automatically  $\sigma$ , the same effect (transition of cylinder to sphere, Ref. [10]) is obtained, but with no connection to physical temperature.

Another point is that the change of the temperature in a real system would, to some extent, influence the density of the melt. We have verified that if smaller values of  $\rho$  are used for larger temperatures, the net effect is only a shift of several degrees in the transition temperature and the general conclusions are not affected.

#### Acknowledgements

Financial support was provided by the Universidad Nacional Autónoma de México (UNAM), PAPIIT project: No. IN101008 and the PASIVE project No. VIASC-102.

#### References

- [1] Kim JK, Lee HH, Gu QJ, Cahng T, Joeng YH. *Macromolecules* 1998;31:4045–8.
- [2] Sakurai S, Momii T, Taie K, Shibayama M, Nomura S, Hashimoto T. *Macromolecules* 1993;26:485–91.
- [3] Leibler L. *Macromolecules* 1980;13:1602–7.
- [4] Fredrickson GH, Helfand EJ. *Chem Phys* 1987;87:697–705.
- [5] Ryu CY, Lodge TP. *Macromolecules* 1999;32:7190–201.
- [6] Sakamoto N, Hashimoto T, Han CD, Kim D, Vaidya NY. *Macromolecules* 1997;30:1621–32.
- [7] Krishnamoorti R, Modi MA, Tse MF, Wang HC. *Macromolecules* 2000;33:3810–7.
- [8] Kimishima K, Koga T, Hashimoto T. *Macromolecules* 2000;33:968–77.
- [9] Krishnamoorti R, Silva AS, Modi MA, Hammouda B. *Macromolecules* 2000;33:3803–9.
- [10] Soto-Figueroa C, Rodríguez-Hidalgo MR, Luis-Vicente, Martínez-Magadán JM. *Macromolecules* 2008;41:3297–304.
- [11] Sakurai S, Kawada H, Hashimoto T, Fetters LJ. *Macromolecules* 1993;26:5796–802.
- [12] Wang CY, Lodge TP. *Macromolecules* 2000;35:6997–7006.
- [13] Foster S, Khandpur AK, Zao J, Bates FS, Hamley IW, Ryan AJ, et al. *Macromolecules* 1994;27:6922–35.
- [14] Khandpur AK, Forster S, Bates FS, Hamley IW, Ryan AJ, Bras W, et al. *Macromolecules* 1995;28:8796–806.
- [15] Hoogerbrugge PJ, Koelman JMVA. *Europhys Lett* 1992;19:155–60.
- [16] Koelman JMVA, Hoogerbrugge PJ. *Europhys Lett* 1993;21:363–8.
- [17] Groot RD, Warren PB. *J Chem Phys* 1997;107(11):4423–35.
- [18] Groot RD, Madden TJ. *J Chem Phys* 1998;108(20):8713–24.
- [19] Groot RD, Madden TJ, Tildesley DJ. *J Chem Phys* 1999;110(19):9739–49.
- [20] Verlet L. *Phys Rev* 1967;159:98–103.
- [21] Accelrys. Material studio release, notes, release 4.3. San Diego: Accelrys Software, Inc.; 2006.
- [22] Fan FC, Olafson BD, Blanco M, Hsu SL. *Macromolecules* 1992;25:3667–76.
- [23] Doi M, Edwards SF. *The theory of polymer dynamics*. Oxford UK: Oxford University Press; 1998.
- [24] Soto-Figueroa C, Rodríguez-Hidalgo MR, Martínez-Magadán JM. *Polymer* 2005;46:7485–93.
- [25] Strobl G. *The physics of polymers*. 2nd ed. Berlin: Springer; 1977.
- [26] Soto-Figueroa C, Rodríguez-Hidalgo MR, Martínez-Magadán JM, Luis-Vicente. *Chem Phys Lett* 2008;460:507–11.